

**Covalent modification of surfaces with porous coordination cages**

Journal:	<i>Journal of Materials Chemistry A</i>
Manuscript ID	TA-ART-08-2023-004662.R1
Article Type:	Paper
Date Submitted by the Author:	21-Sep-2023
Complete List of Authors:	Montone, Christine; Indiana University, Chemistry Dworzak, Michael; University of Delaware, Chemistry and Biochemistry Yap, Glenn P A; University of Delaware, Bloch, Eric; University of Delaware, Chemistry and Biochemistry

## ARTICLE

## Covalent modification of surfaces with porous metal-organic materials

Received 00th January 20xx,  
Accepted 00th January 20xx

Christine M. Montone<sup>a,b</sup>, Michael R. Dworzak<sup>b</sup>, Glenn P. A. Yap<sup>b</sup> and Eric D. Bloch<sup>\*a</sup>

DOI: 10.1039/x0xx00000x

Recent advances in metal-organic frameworks (MOFs) and porous coordination cages (PCCs) have led to their extensive use in various applications due to their tunable properties and exceptional surface areas. To address challenges in harnessing their tunability, surface deposition of MOFs and cages has been investigated. This paper presents efforts in surface attachment of porous cages, leveraging click chemistry, alkylation reactions, and electrostatic approaches. HKUST-1 MOF nanoparticles were covalently tethered to an azide-modified gold surface using copper-catalyzed click chemistry, allowing precise control over the deposited layer. Calixarene and zirconium cages were also attached via click chemistry, providing controlled crystallinity and thickness. Complementary strategies using minimally-functionalized ligands enabled cage attachment to surfaces. These surface-attached porous materials offer versatile approaches for functionalizing surfaces in catalysis, sensing, drug delivery, and other applications, expanding the utility of porous materials in diverse fields. The results demonstrate the feasibility of surface attachment for porous cages.

### Introduction

Advances in the design and synthesis of novel metal-organic frameworks (MOFs) and porous coordination cages (PCCs; cages) have been extensive in recent years. The remarkable tunability of both MOFs and cages, combined with the exceptional surface areas of MOFs and the solution processability of cages,<sup>1</sup> make them highly attractive materials for a wide range of applications across diverse fields. These hybrid porous solids have demonstrated great potential in catalysis,<sup>2</sup> drug delivery,<sup>3,4</sup> tissue engineering,<sup>5</sup> carbon capture,<sup>6</sup> environmental remediation,<sup>7</sup> gas storage,<sup>8</sup> gas separations,<sup>9,10</sup> chemical sensors,<sup>11</sup> and nanodevices,<sup>12</sup> among others.<sup>13</sup> However, harnessing their tuneable properties often requires significant processing, such as compressing into pellets, extrudates, or monoliths for gas storage or separation applications,<sup>14,15,16</sup> or covalent attachment to surfaces for interfacial chemistry-related applications like sensing or electrochemical devices.

To address these challenges, the surface deposition of porous materials, including MOFs and cages, has been under investigation. In some cases, direct growth of MOFs or cages on solid supports has been reported, employing various approaches (Figure 1).<sup>17,18,19,20</sup> Epitaxy, which involves layer-by-layer growth achieved by alternating exposure of a surface to metal and ligand precursors, enables gradual MOF growth

on a targeted surface. Epitaxy typically requires surface modification of the substrate to facilitate the initial seeding of MOF growth. Our research group has successfully demonstrated efficient electrochemical growth of Fe-MIL-101 and Fe-MIL-101-NH<sub>2</sub> on a conductive indium tin oxide surface, which had been electrochemically modified to provide a layer of carboxylic acid groups enabling covalent attachment of the growing MOF.<sup>21</sup> This process also allows for precise control of MOF placement in a patternable manner. In contrast to direct synthesis on a solid support, isolated solids can be deposited onto surfaces using spin coating,<sup>22</sup> with or without a combined epitaxy method,<sup>23,24</sup> to disperse films on various substrates.

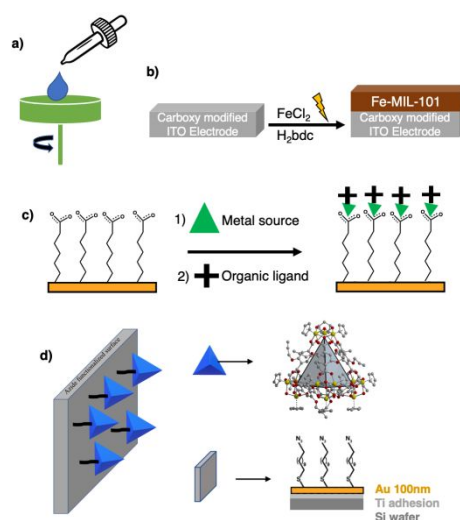


**Fig. 1** a-c) Schemes depicting previously reported porous material surface deposition & thin film growth methods, including spin coating (a), electrochemical surface synthesis (b), epitaxy or layer-by-layer growth (c). Scheme depicting this work covalently attaching cages to an azide-modified gold surface (d).

<sup>a</sup> Department of Chemistry, Indiana University, Bloomington, Indiana 47405, United States. E-mail: edbloch@iu.edu

<sup>b</sup> Department of Chemistry & Biochemistry, University of Delaware, Newark, Delaware 19716

† Electronic Supplementary Information (ESI) available: adsorption isotherms, crystallographic information, spectroscopic data. See DOI: 10.1039/x0xx00000x

These methods can be used independently or in combination to achieve desired film properties. Additionally, thin films and membranes have been obtained using dip coating<sup>25</sup> and drop casting, where a suspension of isolated MOF is added drop-by-drop onto a heated surface, leaving behind a layer of MOF as the solvent evaporates.<sup>26,27</sup> Spray drying, a similar method, involves the deposition of MOF particles onto targeted surfaces by passing a suspension of MOF through a heated orifice using a specified flow rate of inert gas.<sup>28,29</sup> Finally, chemical vapor deposition has been used to deposit MOF films on substrates.<sup>30,31</sup>

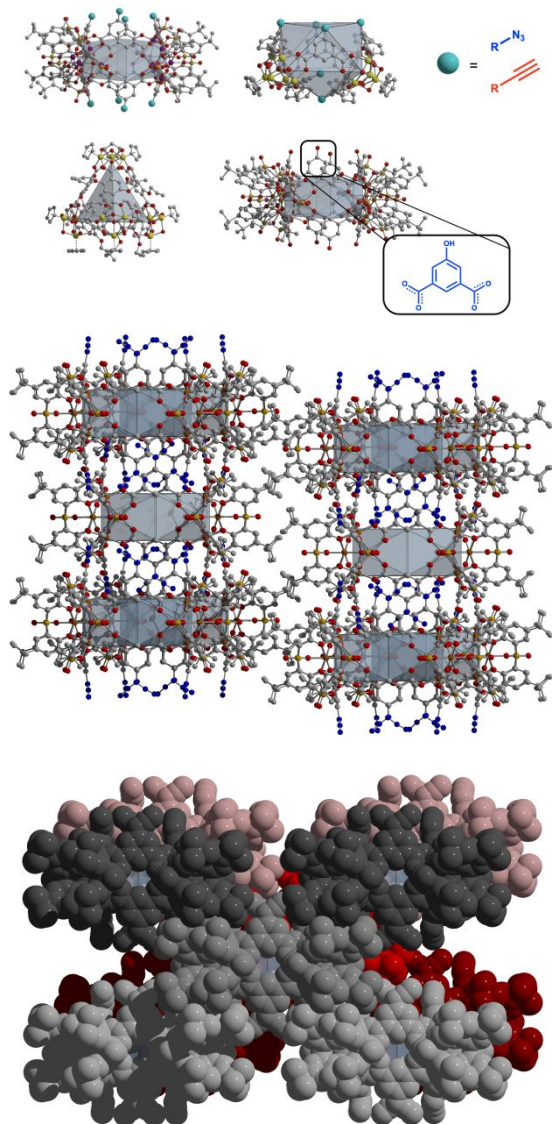


**Fig. 2** Cage materials used in this work, including Mg- or Co-based cages (top left), Zr-based cages (top right) with alkyne or azide functional groups, or Zr-based tetrahedral cages with alkyne functional groups (middle left) for click chemistry reactions with surfaces. Mg-based cage with hydroxy functional groups for alkylation reactions with surfaces. Shaded polyhedra in each cage depicts the pore geometry present in each type of cage. Crystal packing of the Mg-based azide cage (bottom).

Notably, while most surface deposition work has predominantly focused on MOFs, there exists an untapped potential in the realm of porous cages. Despite sharing

structural similarities with MOFs, porous cages have been relatively underexplored in surface deposition studies. This limitation restricts the toolkit available to researchers investigating hybrid metal-organic adsorbents. It is important to note that MOFs are insoluble, which limits post-synthetic control over material properties such as crystallinity and particle size. In contrast, porous cages, owing to their molecular nature and solubility in a range of solvents, offer an additional level of processability. This characteristic can potentially be leveraged to develop innovative surface deposition techniques, thus expanding the repertoire of options for researchers in this field. The solubility of porous cages facilitates solution processing, homogeneous solution-state post-synthetic modification,<sup>32,33,34</sup> and provides control over particle size and crystallinity after synthesis.<sup>35</sup> In this context, this work seeks to address these limitations and explore the potential of porous cages in surface deposition applications. Through a comprehensive investigation, we aim to unveil new strategies for enhancing the accessibility and functionality of these materials in various domains.

For the work presented here, two distinct types of soluble cages were selected. The first is a Type-III sulfonylcalixarene-based cage that can be synthesized with various metals, including cobalt and magnesium.<sup>36,37</sup> These box-like cages feature four metal-calixarene clusters at their vertices bridged by eight organic ligands derived from isophthalic acid, with a 120° angle between coordinating carboxylate groups. This geometry facilitates functionalization at the 5-position of isophthalic acid, where four functional groups are directed "up" on one face of the cage and the remaining four point "down." This bidirectional functional group access ensures consistency and control over the orientation of reactions between the cage and the surface. These cages are anionic with a 4- charge. The second type of cage employed is a zirconium-based cage, which can be synthesized in one of two geometries depending on the dicarboxylate ligand used in their synthesis.<sup>38,39</sup> Both geometries consist of four zirconium clusters capped with cyclopentadienyl rings, connected by six organic carboxylate ligands. In the tetrahedral cage, there is a 180° angle between coordinating carboxylate groups, while the other geometry features a 120° angle between groups. Both ligand sites can be functionalized, resulting in cages with four ligand functional groups pointing "up" and two pointing "down" and towards each other in the window geometry, or with six linear terephthalic acid ligands symmetrically positioned on the edges of each face. Both zirconium cage geometries are cationic, with four counter anions that can be systematically chosen to confer optimized solubility to the cages.

This manuscript presents our efforts in cage surface attachment, utilizing copper-catalyzed azide-alkyne cycloadditions (CuAAC), straightforward alkylation reactions, and simple electrostatic approaches for cage attachment to modified surfaces. Leveraging the solubility and solution processability of cages, as well as our experience in synthesizing various functionalized or charged cages, we

demonstrate that porous cages offer unique advantages for attaching porous products to diverse solid supports.

## Results and Discussion

Given our recent success in utilizing copper catalyzed azide-alkyne cycloaddition (CuAAC) click chemistry to post-synthetically modify porous coordination cages,<sup>40</sup> we targeted click reactions as a facile and rapid way to covalently tether MOFs or cages to diverse surfaces. The modification of surfaces with small-molecules by click chemistry is rather straightforward,<sup>41</sup> an azide or alkyne functionalized surface is reacted with the complementary alkyne or azide-containing molecule under appropriate conditions to afford surface-attached species. In terms of click chemistry involving MOFs, this approach is somewhat limited as the presence of azide or alkyne groups on bridging ligands can interfere with framework formation and the number of such MOFs is limited.<sup>42,43</sup> Similarly, these groups may not be compatible with the bridging ligand used for some materials. HKUST-1, for example, is comprised of trimesic acid ligands and derivatives of this linker to give functionalized HKUST-1 analogues are rare.<sup>44,45</sup> Rather, we targeted the open metal sites for functionalization in the structure. Typically, click chemistry on MOFs has been achieved by integrating clickable groups onto the organic bridging ligands. In this work, we wanted to utilize the copper paddlewheel units in the MOF which can potentially be modified with azide or alkyne containing molecules as the use of *n*-donor ligands to functionalize this site in other porous materials has been achieved in the past. This technique can expand the number of MOFs that can participate in click reactions where ligand modification to incorporate click relevant groups would be challenging or impossible. The reaction of an amine-based small alkyne molecule, propargyl amine, with an azide-functionalized gold surface, prepared by reaction of 11-azido-1-undecanethiol with a 100 nm thick gold layer on a silicon wafer, installs free amines on the surface to potentially coordinate to the axial sites of the copper cations in HKUST-1. We attempted direct surface growth of MOF by subjecting the amine-functionalized surface to the solvothermal conditions that are employed for HKUST-1 synthesis to nucleate MOF growth from the surface. Analysis of the material deposited on the surface in this manner reveals minimal growth with XPS confirming the presence of copper and carbon, but while SEM and grazing incidence X-ray diffraction (GID) revealing an amorphous material. To remedy this, we prepared HKUST-1 for direct post-synthetic surface attachment. In this approach, pre-synthesized HKUST-1 particles were allowed to coordinate and order themselves on the amine-functionalized surface. SEM images and grazing incidence diffraction patterns of both surfaces are shown in Figure 3, where it is clear that the pseudo-epitaxy method produced a less crystalline, less ordered surface coating as compared to covalent tethering of pre-synthesized particles.

To more precisely control the thickness and morphology of the deposited layer, we employed a modified approach where we utilized smaller HKUST-1 particles and attached a coordinating propargyl amine to the nanoparticles prior to deposition. In this regard, synthesized 50-60 nm HKUST-1 nanoparticles were coordinated with propargyl amine, isolated, and characterized by

PXRD. The resulting nanoparticles were compared to the starting HKUST-1 nanoparticles (Fig. S12). Given the retention of crystallinity, CuAAC reaction with an azide-modified gold surface was performed. After several washing steps and sonication of the surface-functionalized material in amide solvent, the sample was dried and imaged by SEM and AFM, Figure 3. With this post-coordination reaction, X-ray photoelectron spectroscopy (XPS) analysis shows the presence of copper and carboxylate-based carbon as expected for this material, Fig. S5. Also of note is the high-resolution XPS spectra for nitrogen, where the peak corresponding to the central azide nitrogen at 404 eV is noticeably absent, with only a peak corresponding to the amine and triazole nitrogen at 400 eV present.

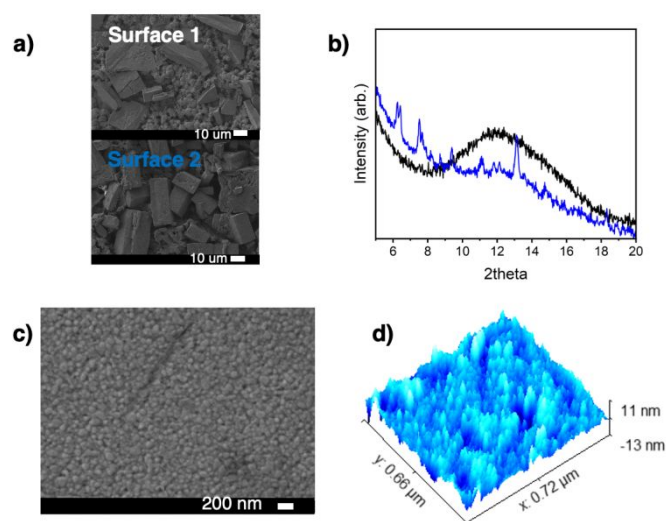


**Fig. 3** a) SEM image of surface 1 where HKUST-1 was solvothermally grown on a gold surface that was modified with an azide followed by click reaction with propargyl amine, & surface 2 where HKUST-1 particles were allowed to deposit on a gold surface that was modified with an azide followed by click reaction with propargyl amine. b) GID patterns of the surfaces from a) with the black trace corresponding to surface 1 & the blue trace corresponding to surface 2. c) SEM image of thin film of HKUST-1 formed from azide modified gold surface after click reaction with propargyl amine-modified HKUST-1 particles. d) AFM map of surface from c.

The transition from targeted solvothermal growth of large particle size MOFs to smaller nanoparticle size afforded significant tunability and control over surface texture, thickness, and homogeneity. Extending this size reduction approach further, the reaction of porous molecules enables even greater control over surface chemistry. Porous coordination cages, being molecular versions of MOFs, are suitable candidates for this purpose, particularly due to their high solubility in organic solvents. Cages offer the potential for more efficient post-synthetic modifications than MOFs due to this added solubility, allowing for enhanced control over particle size, crystallinity, and thickness of the deposited layer. Calixarene-capped cages, which we have previously reported, are excellent candidates as they are synthesized modularly, and our group has developed a facile and rapid CuAAC method for their reaction with small molecules. To explore this, Co calixarene cages containing 5-propargyl isophthalic acid were reacted with a thiol-azide modified gold surface in the presence of copper(II) and a reducing agent. This cyclization click reaction

resulted in the covalent tethering of individual cage units on the surface. After rigorous washing, the functionalized surface was characterized by XPS and AFM, confirming the presence of cobalt, carbon, and sulfur at the appropriate concentrations corresponding to the expected cage composition (Figure S6). The AFM images exhibited a surface texture consistent with the deposition of cage crystallites, with a peak height of just under 5 nm.

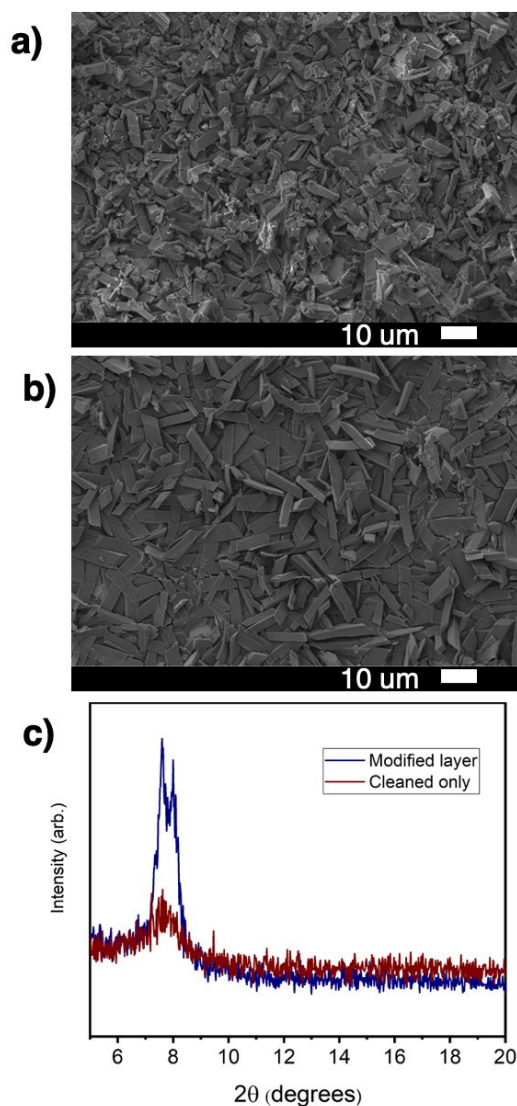


**Fig. 4** a) Co-III ppg cage allowed to crystallize out of DMF on a cleaned, unmodified gold surface. b) Co-III ppg cage allowed to crystallize out of DMF on an azide-modified gold surface that was first subjected to click reaction with Co-III ppg cage. Crystallization conditions were identical between a & b. c) PXRD of both surfaces.

The homogeneity of the surface-bound cage layer makes it a potential nucleation site for the solvothermal or evaporative growth of subsequent cage layers. Leveraging the solubility of the Co 5-ppg calixarene cage, a cleaned, unmodified surface was compared to a surface that had been azide-modified and subsequently reacted to form a Co 5-ppg calixarene clicked layer. A solution of additional Co 5-ppg calixarene cage was allowed to slowly crystallize out of DMF on each surface. The particle size and morphology control of cage materials is a complex multi-factorial process, so in an effort to isolate the surface differences as an

experimental factor, the crystallization conditions were identical between both surfaces. As anticipated, the surface modified with a layer of cage resulted in a thicker and more homogeneous layer. Though the PXRD patterns of cage materials are often amorphous, the pattern of the clicked layer surface exhibited a sharper peak at  $8^\circ$   $2\theta$  compared to the unmodified surface, indicating a more ordered conformation of the crystallized layers. SEM images also revealed regular and ordered crystallites on the clicked layer surface, whereas the unmodified surface exhibited disordered and irregularly shaped and sized crystallites (Figure 4).

Surface-attached cages also offer significant advantages in the preparation of mixed-cage materials, where cages can be deposited in a layer-by-layer fashion using complementary click functional groups. To achieve a mixed-cage surface layer, we initially employed a layer of Co 5-ppg calixarene cage on an azide-modified surface, followed by a layer of Mg 5-azide calixarene cage. After this stepwise click reaction, the surface was characterized by XPS, revealing the presence of both Mg and Co. AFM and SEM images demonstrated a homogeneous textured surface, indicating an even distribution of cage material. Encouraged by the success of covalently tethering Mg and Co calixarene-based cages onto a surface, we aimed to extend the utility of this method to different cage geometries and compositions. Another cage type of interest was a zirconium-based cage composed of six isophthalic acid ligands and four zirconium clusters capped with cyclopentadienyl rings (Figure 2). A second layer-by-layer coating was achieved by first reacting Co 5-ppg calixarene cage followed by a Zr 5-azide cage. XPS analysis of the resulting layer confirmed the presence of both Zr and Co. To determine the thickness of the layers, time-of-flight secondary ion mass spectrometry (TOF-SIMS) was utilized, providing a depth profile with Zr and Co reaching maximum intensities between 25 and 80 seconds of etching. Based on the etch pit depth measurements, assuming a constant etch rate, the thickness of the cage layers was determined to be 50 nm.

Although CuAAC click chemistry can be widely applied to various materials, the requirement of an azide or alkyne functional group on both the material and surface limits the scope of this chemistry, particularly when either the surface or the MOF or cage is incompatible with these functional groups. To overcome this limitation, we explored complementary modification routes using minimally-functionalized ligands. Our previous work demonstrated that hydroxide- or amine-functionalized cages can be post-synthetically modified by reacting them with acyl chlorides or alkyl halides to yield amide, ester, or ether-functionalized cages. This approach is highly applicable to surface functionalization when appropriately functionalized modified surfaces are available. In this study, we reacted a gold surface with 11-bromoundecan-1-thiol to attach alkyl halides to the support, as confirmed by XPS. Considering our frequent use of alkylation reactions between hydroxy-functionalized ligands and alkyl halides to synthesize various ether-functionalized ligands, we selected another Mg calixarene cage synthesized with 5-hydroxy isophthalic acid for this reaction. Calixarene-based cages are known for their exceptional stability among porous coordination cages and exhibit excellent hydrolytic, thermal, and chemical stability. The box-like structure of Mg 5-OH calixarene cage is shown in Figure 2, with eight accessible

ligands arranged such that four point "up" and four point "down." This cage was synthesized solvothermally by reacting t-butyl sulfonyl calix[4]arene,  $\text{MgCl}_2$ , and 5-hydroxy isophthalic acid in DMF. The subsequent alkylation reaction was modified from a typical alkoxy ligand synthesis and performed using the bromide-modified gold surface.

In this reaction, a DMF solution of Mg 5-OH calixarene cage was heated at 65°C for 18 hours in the presence of the thiol bromide-modified gold surface. After thorough washing, XPS spectra confirmed the presence of Mg and the absence of bromine on the surface. SEM and AFM imaging (Figures S3, S32, S41, and S46) displayed a homogeneous and textured surface, indicative of a complete surface reaction with the cage material. As the films produced by these methods are very thin (<20 nm), high-resolution spectroscopy techniques were required to verify the presence of cage material on each surface. While ATR-IR is typically useful for identifying cage or MOF materials in bulk powder or thick films, it was unable to detect any cage material on the surfaces due to their thin nature. NanoIR, which relies on a photothermal IR effect coupled with high-resolution atomic force microscopy, was employed for films in the sub-20 nm regime. Figure S46 presents a comparison between the ATR-IR of bulk Mg cage powder (blue) and the NanoIR of the reacted surface (black). The broad IR signals observed in the NanoIR spectra of the thin films were a consequence of their near detection limit thickness.

In the absence of reactive functional groups on cages, simple electrostatic interactions can also be employed to tether cages, particularly charged cages, to surfaces. Carboxylate-modified surfaces have been demonstrated to serve as reliable anchor points for the surface growth of MOFs, where carboxylate-metal or hydrogen bonding interactions result in robust films. In our study, we targeted a gold surface modified with 11-mercaptoundecanoic acid, as the dangling carboxylate groups on this molecule can act as anions for cationic cages. By deprotonating the carboxylic acid on the surface with sodium carbonate, followed by cation exchange between  $\text{Na}^+$  and a cationic cage, surface-attached cage formation can be achieved. The selected material for this exchange was a Zr-based tetrahedral cage synthesized with 2,5-dimethyl terephthalic acid. For ease of ion exchange monitoring and to enhance solubility, this 4+ charged cage was synthesized with triflate counter-anions by solvothermally reacting bis(cyclopentadienyl) zirconium (IV) bis trifluoromethanesulfonate and 2,5-dimethyl terephthalic acid in DMF and water. After a short ion exchange time (< 30 minutes), during which a deuterated methanol solution of the cage was allowed to react with the carboxylate surface, the surface was washed twice with deuterated methanol. The resulting solution was analyzed by  $^{19}\text{F}$  and  $^1\text{H}$  NMR, and the spectra of each MeOD wash were compared to a MeOD solution of unreacted cage. The first wash showed peaks in both the proton and fluorine spectra, indicating the presence of both cage and triflate anion. In contrast, the second wash showed no remaining cage or triflate anion, indicating a well-cleaned surface. XPS analysis of the ion-exchanged surface revealed no detectable fluorine but confirmed the presence of Zr. The combination of XPS and NMR confirmed that an ion exchange reaction occurred, resulting in the electrostatic attachment of a Zr-based cage on the surface, forming a salt with the carboxylate-modified gold surface.

## Conclusions

In conclusion, we have successfully demonstrated various strategies for surface attachment of porous coordination cages (PCCs) and metal-organic frameworks (MOFs). Leveraging click chemistry, we achieved covalent tethering of HKUST-1 MOF nanoparticles to an azide-modified gold surface, enabling precise control over the deposited layer's thickness and morphology. Calixarene-based cages and zirconium-based cages were also successfully attached to surfaces using click chemistry, providing controlled crystallinity and thickness. Additionally, complementary modification routes using minimally-functionalized ligands allowed for the attachment of cages to surfaces, offering alternative strategies when click chemistry is not applicable. Overall, the surface attachment of PCCs and MOFs presents a versatile approach to functionalize surfaces for various applications. Our findings open up new possibilities in catalysis, sensing, drug delivery, and other fields. Further investigations into surface attachment techniques will continue to advance the utilization of porous materials in diverse industrial and scientific applications.

## Conflicts of interest

There are no conflicts to declare.

## Acknowledgements

This research was supported by the National Science Foundation (NSF) through the University of Delaware Materials Research and Engineering Center, DMR-2011824-The Center for Hybrid, Active, and Responsive Materials (CHARM). We thank Gerald Poirier and Jing Qu of the Advanced Materials Characterization Lab at the University of Delaware for their expertise and assistance with AFM and NanoIR experiments. XPS analysis was performed with the instrument sponsored by the National Science Foundation under grant No. CHE-1428149. ToF-SIMS analysis was performed with the instrument sponsored by the National Science Foundation under grant No. DMR-2116754.

## References

- 1 M. M. Deegan, A. M. Antonio, G. A. Taggart and E. D. Bloch, *Coord. Chem. Rev.*, 2021, **430**, 213679.
- 2 R. J. Comito, K. J. Fritzsche, B. J. Sundell, K. Schmidt-Rohr and M. Dinca, *J. Am. Chem. Soc.*, 2016, **138**, 10232-10237.
- 3 G. E. Decker, Z. Stillman, L. Attia, C. A. Fromen and E. D. Bloch, *Chem. Mater.*, 2019, **31**, 4831-4839.
- 4 X. Chen, Y. Zhuang, N. Rampal, R. Hewitt, G. Divitini, C. A. O'Keefe, X. Liu, D. J. Whitaker, J. W. Wills, R. Jugdaohsingh, J. J. Powell, H. Yu, C. P. Grey, O. A. Scherman and D. Fairen-Jimenez, *J. Am. Chem. Soc.*, 2021, **143**, 13557-13572.
- 5 M. Shyngys, J. Ren, X. Liang, J. Miao, A. Blocki and S. Beyer, *Front. Bioeng. Biotechnol.*, 2021, **9**, 603608.
- 6 T. M. McDonald, W. R. Lee, J. A. Mason, B. M. Wiers, C. S. Hong and J. R. Long, *J. Am. Chem. Soc.* 2012, **134**, 7056-7065.
- 7 H. Kaur, M. Venkateswarulu, S. Kumar, V. Krishnan and R. R. Koner, *Dalton Trans.* 2018, **47**, 1488-1497.
- 8 O. K. Farha, I. Eryazici, N. C. Jeong, B. G. Hauser, C. E. Wilmer, A. A.

- Sarjeant, R. Q. Snurr, S. T. Nguyen, A. O. Yazaydin and J. T. Hupp, *J. Am. Chem. Soc.* 2012, **134**, 36, 15016-15021
- 9 O. T. Qazvini, R. Babarao and S. G. Telfer, *Nature Communications*, 2021, **12**, 197.
- 10 E. D. Bloch, W. L. Queen, R. Krishna, J. M. Zadrozny, C. M. Brown and J. R. Long, *Science* **2012**, *335*, 1606-1610.
- 11 J. E. Ellis, S. E. Crawford and K. Kim. *Mater. Adv.* 2021, **2**, 6169-6196.
- 12 P. Falcaro, K. Okada, T. Hara, K. Ikigaki, Y. Tokudome, A. Thornton, A. Hill, T. Williams, C. Doonan and M. Takahashi. *Nature Materials*, 2017, **16**, 342-348.
- 13 A. R. M. Silva, J. Y. N. H. Alexandre, J. E. S. Souza, J. G. Lima Neto, P. G. de Sousa Junior, M. V. P. Rocha and J. C. S. dos Santos. *Molecules*, 2022, **27**, 4529.
- 14 T. Tian, Z. Zeng, D. Vulpe, M. E. Casco, G. Divitini, P. A. Midgley, J. Silvestre-Albero, J. Tan, P. Z. Moghadam and D. Fairen-Jimenez. *Nature Materials*, 2017, **17**, 174-179.
- 15 B. Yeskendir, J. Dacquain, Y. Lorgouilloux, C. Courtois, S. Royer and J. Dhainaut, *Mater. Adv.*, 2021, **2**, 7139-7186.
- 16 F. Figueira, R. F. Mendes, E. M. Domingues, P. Barbosa, F. Figueiredo and F. A. A. Paz, J. Rocha, *Appl. Sci.* 2020, **10**, 798.
- 17 A. M. Beiler, B. D. McCarthy, B. A. Johnson and S. Ott, *Nature Communications*, 2020, **11**, 5819.
- 18 D. Zacher, O. Shekhah, C. Woll and R. A. Fischer, *Chem. Soc. Rev.*, 2009, **38**, 1418-1429.
- 19 N. Campagnol, I. Stassen, K. Binnemans, D. E. de Vos and J. Fransaer, *J. Mater. Chem. A*, 2015, **3**, 19747-19753.
- 20 A. L. Semrau, Z. Zhou, S. Mukherjee, M. Tu, W. Li and R. A. Fischer, *Langmuir*, 2021, **37**, 6847-6863.
- 21 W. Wu, G. E. Decker, A. E. Weaver, A. I. Arnoff, E. D. Bloch and J. Rosenthal, *ACS Cent. Sci.* 2021, **8**, 1427-1433.
- 22 L. D. Sappia, J. S. Tuninetti, M. Ceolin, W. Knoll, M. Rafti and O. Azzaroni, *Glob. Chall.*, 2020, **4**, 1900076.
- 23 J. Liu, O. Shekhah, X. Stammer, H. K. Arslan, B. Liu, J. Schüpbach, A. Terfort, C. Wöll, *Materials*, 2012, **5(9)**, 1581-1592.
- 24 M. Drost, F. Tu, L. Berger, C. Preischl, W. Zhou, H. Gliemann, C. Woll and H. Marbach, *ACS Nano*, 2018, **12**, 3825-3835.
- 25 A. M. Mosier, H. L. W. Larson, E. R. Webster, M. Ivos, F. Tian and L. Benz, *Langmuir*, 2016, **32**, 2947-2954.
- 26 C. M. Doherty, G. Greci, R. Ricco, J. A. Mardel, J. Reboul, S. Furukawa, S. Kitagawa, A. J. Hill and P. Falcaro, *Adv. Mater.* 2013, **25**, 4701-4705.
- 27 Y. Miao, and M. Tsapatsis, *Chem. Mater.* 2021, **33**, 754-760.
- 28 R. Zheng, Z. Fu, W. Deng, Y. Wen, A. Wu, X. Ye and G. Xu, *Angew. Chem.*, 2022, **61**, 43.
- 29 J. Troyano, C. Camur, L. Garzon-Tovar, A. Carne-Sanchez, I. Imaz and D. Maspoch, *Acc. Chem. Res.*, 2020, **53**, 6, 1206-1217.
- 30 F. J. Claire, M. A. Solomos, J. Kim, G. Wang, M.A. Siegler, M. F. Crommie and T. J. Kempa, *Nature Communications*, 2020, **11**, 5524.
- 31 W. Li, P. Su, Z. Li, Z. Xu, F. Wang, H. Ou, J. Zhang, G. Zhang and E. Zeng, *Nature Communications*, 2017, **8**, 406.
- 32 M. L. Schneider, A. W. Markwell-Heys, O. M. Linder-Patton and W. M. Bloch, *Front. Chem.* 2021, **9**, 696081.
- 33 G. A. Taggart, A. M. Antonio, G. R. Lorzing, G. P. A. Yap, and E. D. Bloch, *ACS Appl. Mater. Interfaces* **2020**, *12*, 24913-24919.
- 34 D. Nam, J. Huh, J. Lee, J. H. Kwak, H. Y. Jeong, K. Choi and W. Choe, *Chem. Sci.* 2017, **8**, 7765.
- 35 D. Zhang, T. K. Ronson, Y. Zou and J. R. Nitschke, *Nature Reviews*, 2021, **5**, 168-182.
- 36 F. Dai, D. C. Becht and Z. Wang, *Chem. Comm.*, 2014, **50**, 5385.
- 37 M. R. Dworzak, M. M. Deegan, G. P. A. Yap and E. D. Bloch, *Inorg. Chem.*, 2021, **60**, 5607-5616.
- 38 A. J. Gosselin, G. E. Decker, B. W. McNichols, J. E. Baumann, G. P. A. Yap, A. Sellinger, E. D. Bloch and *Chem. Mater.* 2020, **32**, 5872-5878.
- 39 S. Du, X. Yu, G. Liu, M. Zhou, E. M. El-Sayed, Z. Ju, K. Su and D. Yuan, *Cryst. Growth Des.*, 2021, **21**, 692-697.
- 40 M. R. Dworzak, C. M. Montone, N. I. Halaszynski, G. P.A. Yap, C. J. Kloxin and E. D. Bloch, *Chem. Comm.* 2023, **59**, 8977.
- 41 M. G. Williams and A. V. Teplyakov, *Appl. Surf. Sci.*, 2018,
- 42 Y. Goto, H. Sato, S. Shinkai and K. Sada, *J. Am. Chem. Soc.* 2008, **130**, 14354-14355.
- 43 Y. Zhang, B. Gui, R. Chen, G. Hu, Y. Meng, D. Yuan, M. Zeller and C. Wang, *Inorg. Chem.* 2018, **57**, 2288-2295.
- 44 Y. Cai, A. R. Kulkarni, Y. Huang, D. S. Sholl and K. Walton, *Cryst. Growth Des.*, 2014, **14**, 11, 6122-6128.
- 45 S. Zong, S. Huang, X. Shi, C. Sun, S. Xu, P. Ma and J. Wang, *Dalton Trans.* 2020, **49**, 12610-12621.